JOURNAL OF MATERIALS SCIENCE: MATERIALS IN MEDICINE 6 (1995) 113–119

Spectroscopic characterization of passivated titanium in a physiologic solution

J. L. ONG*, L. C. LUCAS
University of Alabama at Birmingham, Department of Biomedical Engineering, University Station, Birmingham, Alabama 35294, USA

G. N. RAIKAR, R. CONNATSER, J. C. GREGORY
University of Alabama in Huntsville, Surface Science Laboratories, College of Science, Huntsville, Alabama 35899, USA

Titanium (Ti) has been used for many biomedical applications. Surface characteristics of titanium devices are critical to their success. In this study, Raman spectroscopy and X-ray photoelectron spectroscopy (XPS) were used to analyse Ti surfaces prior to immersion in alpha-modification of Eagle's medium (α-MEM). The ionic constituents deposited onto Ti surfaces after *in vitro* exposure to α-MEM were investigated using XPS and Fourier transform infrared spectroscopy (FTIR). Surface studies revealed an amorphous oxide layer on the Ti surface, with a chemistry similar to TiO_2. However, after exposure to the physiologic solution for 12 days, dynamic changes in surface chemistry were observed. Ions such as phosphorus (P) and calcium (Ca) were increasingly deposited as amorphous fine crystalline calcium-phosphate (Ca–P) compounds, having a Ca/P ratio of 1.2 and a chemistry similar to brushite.

1. Introduction

Titanium (Ti) has been a material of choice for many orthopaedic and dental implant devices. A primary reason for using Ti relates to its biocompatibility [1–2]. Titanium ions, when released from implants, have generally been considered to be compatible with adjacent tissues [3–5].

Prior to the attachment of bony tissue to a titanium implant, the prosthesis first encounters various proteins and ligands [6–7]. Biomolecules from the body fluid have been suggested to be continuously adsorbed on the implant surface and exchanged for desorbing proteins or displaced proteins in the adsorbed layer [8]. These interfacial interactions can occur within a narrow interfacial zone of less than 1 nm, and it is these initial interfacial interactions that determine initial bony attachment [6]. Depending on surface conditions, different rates of cellular attachment have been observed *in vitro*. These differences have been attributed to varying surface chemistries of the titanium oxides on the titanium surface [9].

Since surface phenomena play a critical role in biological performance, the behaviour of titanium surfaces in the biological environment needs to be critically evaluated. It has been reported that inorganic deposition on a surface occurs *in vivo* [10, 11]. Previous investigations have also reported the deposition of inorganic constituents during *in vitro* laboratory experiments [12–14]. However, depending on the type of surface and the time in contact with the biological environment, inorganic deposits can differ in structure and chemistry. Thus, the goal of this study was to characterize and evaluate Ti surfaces before and after exposure to a physiologic solution using Raman spectroscopy, X-ray photoelectron spectroscopy (XPS) and Fourier transformation infrared spectroscopy (FTIR).

2. Materials and methods

2.1. Substrate material

Ti grade 2 (ASTM F76) was the substrate for all studies. The chemical composition of Ti grade 2 was obtained from the manufacturer (Metal Samples, Munford, AL, USA) and is shown in Table I. The Ti samples were mechanically ground with 240, 400 and 600 grit silicon carbide and polished with 1 μm and 0.3 μm alumina powders. They were then ultrasonically degreased in benzene, acetone and ethanol for 10 min each, with deionized water rinsing between

TABLE I Chemical composition of Ti grade 2 samples

Elements	Weight percentage
C	0.023
Fe	0.16
N	0.006
O	0.13
Ti	Balance

* Present address: The University of Texas Health Science Center at San Antorio, Department of Restorative Dentistry, Division of Biomaterials, 7703 Floyd Curl Drive, San Antorio, TX 78284-7890, USA

0957–4530

application of each solvent. A passivation procedure involved exposing Ti samples to a 40% volume nitric acid solution at room temperature for 30 min (ASTM F86–76). After each surface treatment, samples were rinsed with deionized water. The samples were then sterilized under UV light for a minimum of 24 h prior to conducting the immersion study.

2.2. Immersion study

Ti samples were placed in 12-well tissue culture plates and immersed in 1 ml alpha-modification of Eagle's medium (α-MEM) from Cellgro (VA, USA) for a period of 3 h, 3 days, 6 days, 9 days and 12 days. The pH of the α-MEM was 7.4 and media were changed every 3 days. The experiment was conducted in a humidified atmosphere (95% air and 5% CO_2) at 37 °C.

2.3. Raman spectroscopy

Raman spectroscopy was used to evaluate the structural composition of the Ti surface prior to immersion in solution, and was compared to a standard rutile TiO_2 powder (New Jersey Zinc Co., New York). Analysis was performed using a Spectra-Physics 171 argon-ion laser ($\lambda = 488$ nm). The laser power was set at 400 mW during analyses, and passed through a diffraction grating, thereby allowing the final laser power on the sample to be 100 mW. A Spex 1401 double monochromator was used with a slit height of 10 mm and slit width of 225, 250 and 225 μm. After dispersion, the frequency-shifted light was detected by a cooled RCA C31034 photomultiplier tube, and a Stanford Instruments SR400 gated photon counter. All samples were analysed with a resolution of 5 cm^{-1} and a scan rate of 1 cm^{-1}/channel/s for a range of 100 cm^{-1} to 800 cm^{-1}.

2.4. X-ray photoelectron spectroscopy (XPS)

XPS was performed on a Perkin-Elmer 5400 system at a base pressure of less than 10^{-7} Pa. Duplicate samples prior to immersion and after immersion were analysed using a take-off angle of 45°. Commercially available brushite (Aldrich Chemical Co., Milwaukee, Wisconsin, USA), hydroxyapatite (CAM Implants, Arvada, Colorado, USA), and TiO_2 rutile single crystal were used as standards. All surface spectra over a range of 0–1100 eV were obtained using MgK_α radiation (1253.6 eV) at 15 kV and 20 mA. The pass energy used for obtaining the surface spectra was 90 eV. Relative atomic concentrations for all identified elements were quantified from the multiplex spectra (a pass energy of 18 eV) using peak areas and elemental sensitivity factors obtained from the Physical Electronics (Perkin-Elmer) 5400 spectrometer. Using least mean square analyses, the Ca/P ratio and atomic concentrations of different elements at different times were statistically evaluated. High-resolution spectra of C 1s, Ti 2p, O 1s, Ca 2p, and P 2p were collected with a pass energy of 9 eV. From the high-resolution spectra, peak separation between Ti 2p doublets, full width at half maximum (FWHM) for Ti $2p_{3/2}$ and Ca $2p_{3/2}$, and deconvolution of O 1s, C 1s and P 2p spectrum using a Gaussian–Lorentzian model were performed. Photoelectron peak positions were corrected for charging by referencing to the adventitious C 1s peak at 284.6 ± 0.4 eV.

2.5. Fourier transformation infrared spectroscopy (FTIR)

A Mattson Research Series 1 FTIR spectrometer was used to determine the presence of phosphates (PO_4) on Ti surfaces after immersion in α-MEM. Using a resolution of 4 cm^{-1}, and a scan number of 12000, duplicate Ti samples from each time period were analysed using a 75° grazing angle. Gaussian–Lorentzian curve fitting was performed on the PO_4 absorbance band in the range 900 cm^{-1} to 1300 cm^{-1}.

3. Results

3.1. Raman spectroscopy

Fig. 1 shows the surface scan of a Ti sample and the rutile TiO_2 standard. No distinguishable vibration mode was observed for the Ti surface (Fig. 1), whereas vibration modes at 141.5 cm^{-1}, 220 cm^{-1}, 444 cm^{-1}, 514 cm^{-1}, and 608 cm^{-1} were observed for the rutile TiO_2 standard.

3.2. XPS analyses prior to immersion

Surface contaminants such as carbon (C), silicon (Si) and aluminum (Al) were observed during XPS analyses. The atomic concentrations of Al was 1–3% whereas Si was in the range 1–2%. The nitrogen (N 1s) peak was found to have a binding energy of 400 eV which can be attributed to the nitrogen present in the organic molecules in the surface contamination layer. The relative concentration of N was less than 2%.

Fig. 2 shows the high-resolution C 1s peak curve fitted by three components. The dominant component

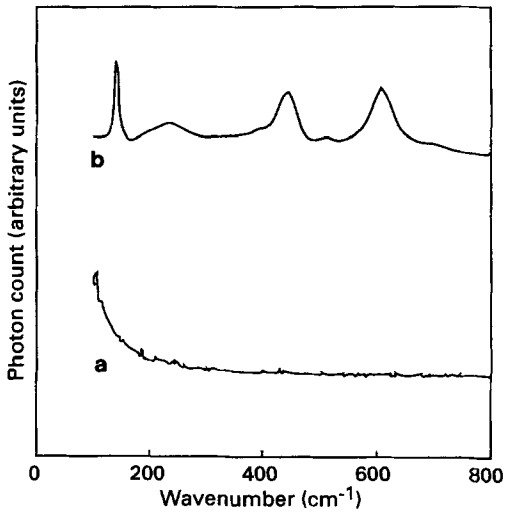

Figure 1 Representative Raman spectra showing an amorphous Ti oxide on Ti surface (a) and a rutile TiO_2 standard (b).

at 284.6 eV is attributed to hydrocarbons (C–C and C–H bonded carbon). Two other components at higher binding energies (286.1 eV and 288.1 eV) were also observed. The relative concentrations of carbon on all surfaces was in the range 21–36%.

The high-resolution Ti 2p spectrum shown in Fig. 3 is representative of the Ti surfaces as well as the TiO_2 single crystal standard. The binding energies of Ti $2p_{1/2}$ Ti $2p_{3/2}$, with peak separation between these two peaks are shown in Table II. These peak positions were not statistically different from the TiO_2 standard. However, some differences in the FWHM were determined at Ti $2p_{3/2}$. The FWHM for the Ti samples was 1.3 eV whereas the FWHM at Ti $2p_{3/2}$ for the TiO_2 single crystal standard was 1.1 eV.

Fig. 4 shows a typical high-resolution spectrum of O 1s obtained for the Ti samples as well as the TiO_2 single crystal standard. The spectrum was deconvoluted into three components. Although no statistical difference in the peak position was observed, differences in the distribution of oxygen species for Ti surfaces and rutile TiO_2 standard were observed (Table III). Differences in the distribution of oxygen species could partly be due to the differences in the concentration of contaminations present on these surfaces.

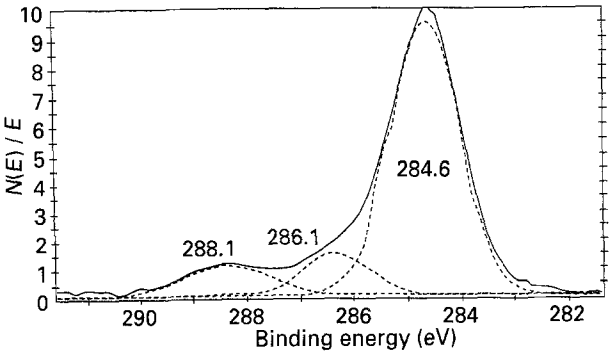

Figure 2 Representative XPS high-resolution spectrum of C 1s prior to immersion in α-MEM.

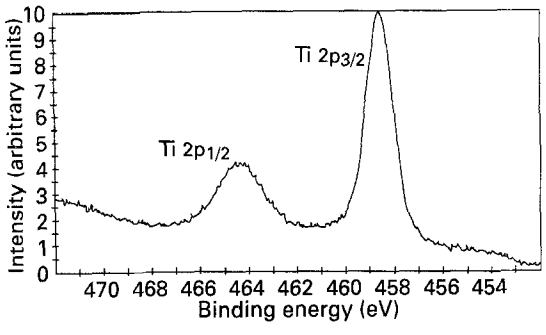

Figure 3 Representative XPS high-resolution spectrum of Ti 2p prior to immersion in α-MEM.

TABLE II Binding energies and peak separation of Ti 2p over time in α-MEM. The standard deviation for binding energies of each component is ± 0.2 eV

Ti sample	Binding energy (eV)		Peak separation (eV)[a]
	Ti $2P_{1/2}$	Ti $2p_{3/2}$	
TiO_2 single crystal[b]	464.0	458.2	5.8
Prior to immersion	464.2	458.4	5.8
3 h immersion	464.0	458.3	5.7
3 days immersion	464.1	458.3	5.8
6 days immersion	464.0	458.1	5.9
9 days immersion	464.0	458.3	5.7
12 days immersion	463.7	458.0	5.7

[a] Peak separation between Ti $2p_{1/2}$ and Ti $2p_{3/2}$
[b] One TiO_2 single crystal standard analysed

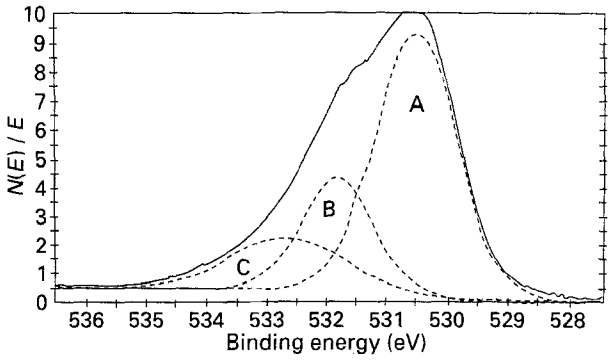

Figure 4 Representative XPS high-resolution spectrum of O 1s prior to immersion in α-MEM. A = 529.8 eV; B = 531.0 eV; C = 532.3 eV.

3.3. XPS analyses after immersion

In addition to the presence of Ti, O, C, N, Al and Si, the presence of other ionic deposits such as phosphorus and calcium were also observed on the Ti surfaces immersed in α-MEM (Fig. 5). Not included in Fig. 5 were trace amounts of nitrogen, aluminum, silicon, chlorine and sodium for all Ti samples immersed in α-MEM. Concentrations of all these trace elements were less than 3%.

The atomic concentrations of Ca and P were observed to increase with time in solution. Table IV shows the average Ca/P ratio with time on the Ti samples after immersion in solution. The Ca/P ratio gradually increased from 0.5 ± 0.4 after 3 h in solution to 1.2 ± 0.1 after 12 days immersion. No statistical difference in the Ca/P ratio was observed between 9 and 12 days. However, the Ca/P ratio was significantly higher at days 9 and 12 than days 3 and 6. Furthermore, in Fig. 5, a decrease in the Ti concentration over time in solution was observed, indicating an increase in the thickness of Ca–P deposits. This decrease in Ti was also reflected in the atomic concentration of O over time in solution, since most of the O was bound to Ti as TiO_2. No statistical difference in the C concentration was observed throughout the 12 day study.

High-resolution spectra of Ti 2p and C 1s obtained after immersion were similar to the spectra prior to immersion. The peak positions of Ti 2p after immersion is shown in Table II. Peak positions and peak separation for Ti 2p after immersion were not significantly different to those for the TiO_2 single crystal standard.

The O 1s high resolution spectra after immersion as well as the O 1s on Ti surfaces prior to immersion were curve fitted with three components (Fig. 6). As

TABLE III Relative distribution (± 1 SD) of different components for O 1s over time in solution. The binding energy of each component is in parenthesis. The standard deviation for binding energies of each component is ± 0.2 eV

Ti Sample	Relative distribution of O 1s concentration (%)		
	Component A (529.8 eV)	Component B (531.0 eV)	Component C (532.3 eV)
TiO_2 single crystal[a]	66.5	5.28	28.24
Prior to immersion	70.4 ± 0.6	12.6 ± 0.3	16.9 ± 0.9
3 h immersion	60.6 ± 0.4	25.5 ± 4.8	13.9 ± 4.4
3 days immersion	48.0 ± 9.2	34.0 ± 12.5	18.1 ± 3.3
6 days immersion	49.9 ± 13.3	34.6 ± 12.6	15.5 ± 0.7
9 days immersion	32.0 ± 7.4	46.4 ± 11.4	21.6 ± 4.1
12 days immersion	12.1 ± 6.7	67.5 ± 3.6	20.4 ± 3.0

[a] One TiO_2 single crystal standard analysed

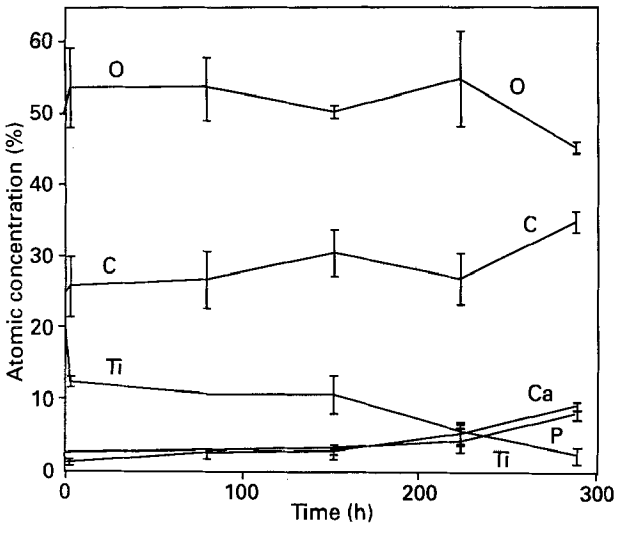

Figure 5 Atomic concentration of various elements after immersion in α-MEM over time.

TABLE IV CA/P ratio of Ti immersed in α-MEM over time

Time	CA/P ratio ± 1 SD
3 h	0.5 ± 0.4
3 days	0.9 ± 0.3
6 days	0.8 ± 0.1
9 days	1.3 ± 0.1
12 days	1.2 ± 0.1

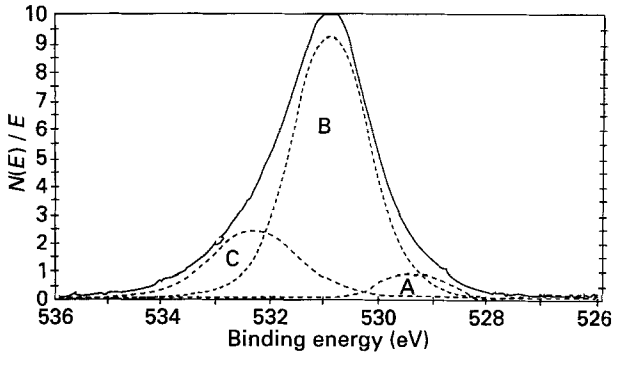

Figure 6 Representative XPS high-resolution spectrum of O 1s after immersion in α-MEM. A = 529.8 eV; B = 531.0 eV; C = 532.3 eV.

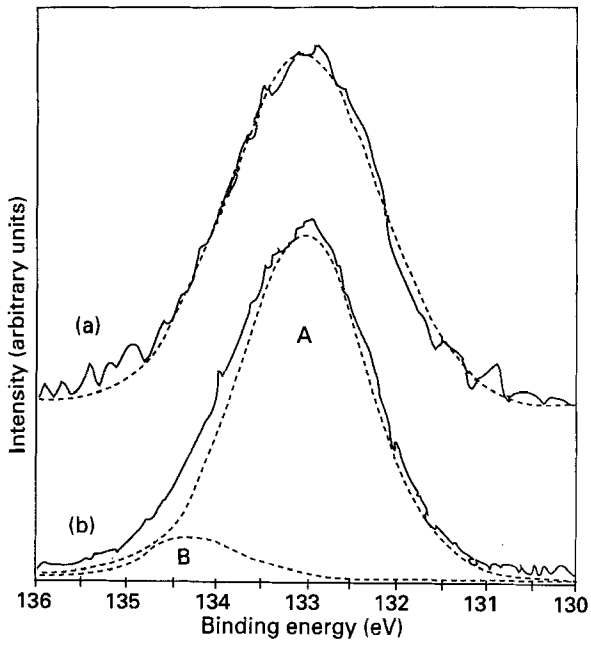

Figure 7 Representative XPS high-resolution spectrum of P 2p: (a) after immersion for 3 h to 3 days in α-MEM; (b) after immersion for 6 to 12 days in α-MEM.

observed from Table III, the relative distribution of O 1s concentration at component A and B changed with time in solution, indicating a dynamic surface. All values were significantly different from the rutile TiO_2 standard. However, the relative concentrations of component C were not statistically altered over time in solution when compared to Ti samples prior to immersion and the TiO_2 single crystal standard.

The high-resolution P 2p spectra were observed to be symmetric for 6 days of the immersion study (Fig. 7a). After 6 days immersion, the P 2p spectra was curve fitted with two components (Fig. 7b). This asymmetry in P 2p spectra was also observed for the brushite and hydroxyapatite standards, which were also curve fitted with two components. Comparing the binding energies of each component and their relative distribution (Table V), the deposited Ca–P compounds after 6 days immersion were observed to have a chemistry similar to the brushite standard.

No chemical shift in the high-resolution Ca 2p peak was observed in this study. Peak symmetry was evident for all high-resolution Ca 2p spectra, with Ca $2p_{3/2}$

TABLE V Relative distribution (± 1 SD) of different components for P 2p over time in solution. The binding energy of each component is in parenthesis. The standard deviation for binding energies of each component is ± 0.2 eV

Ti sample	Relative distribution of P 2p concentration (%)	
	Component A	Component B
Hydroxyapatite standard[a]	91.6 (132.8 eV)	8.4 (133.8 eV)
Brushite standard[a]	93.4 (133.2 eV)	6.6 (134.5 eV)
3 h immersion	100 (132.9 eV)	–
3 days immersion	100 (133.1 eV)	–
6 days immersion	82.6 ± 2.6 (133.2 eV)	17.4 ± 2.6 (134.4 eV)
9 days immersion	85.3 ± 3.5 (133.4 eV)	14.7 ± 3.5 (134.4 eV)
12 days immersion	87.9 ± 3.47 (133.1 eV)	12.1 ± 3.4 (134.3 eV)

[a] One hydroxyapatite and brushite standard analysed

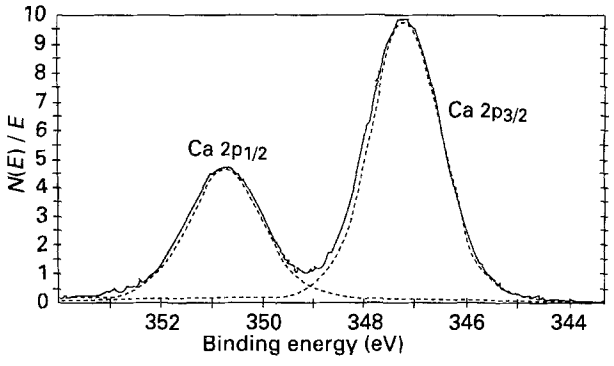

Figure 8 Representative XPS high-resolution spectrum of Ca 2p after immersion for in α-MEM.

at 347.1 eV and Ca $2p_{1/2}$ at 350.7 eV (Fig. 8). The FWHM value of Ca $2p_{3/2}$ for immersed Ti samples was 1.7 eV whereas the FWHM value of Ca $2p_{3/2}$ for the brushite and hydroxyapatite standards was 1.4 eV. The relatively large FWHM value for Ca $2p_{3/2}$ (FWHM = 1.7) on the Ti surfaces compared to the hydroxyapatite (FWHM = 1.4) and brushite standards (FWHM = 1.4) probably indicated a lower degree of crystallinity, or that an amorphous calcium phosphate compound was deposited on the Ti surfaces.

3.4. FTIR

Fig. 9 shows a representative PO_4 absorbance band in the range 900 cm^{-1} to 1300 cm^{-1}. The wide PO_4 absorbance band was deconvoluted and curve fitted with nine components (954 cm^{-1}, 987 cm^{-1}, 1022 cm^{-1}, 1057 cm^{-1}, 1086 cm^{-1}, 1116 cm^{-1}, 1153 cm^{-1}, 1182 cm^{-1} and 1209 cm^{-1}). These nine band positions were similar for all Ti surfaces irrespective of immersion time.

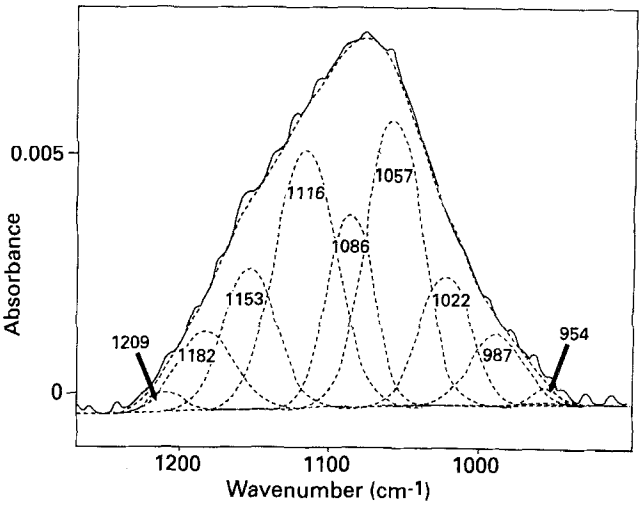

Figure 9 Representative FTIR spectrum of PO_4 absorbance band with an overlay of the contour, and the individual components as determined by curve fitting.

4. Discussion

Evaluating the physico-chemical properties of Ti in contact with body fluids becomes critical since Ti is commonly used for medical devices. Ti is known to exhibit excellent corrosion resistance because of its readiness to form a passive oxide film. Furthermore, there are already investigations on the nature of Ti oxides formed under various sterilization treatments as well as the stability of oxide films in solution [15–19]. However, the deposition of ionic constituents from the solution to Ti surfaces are also important and these deposits may influence cellular behaviour [9, 20, 21].

From Raman spectroscopy, no distinguishable vibration mode was observed on the Ti surfaces. This suggests an amorphous oxide on the passivated Ti surfaces, an observation that has been also made by other investigators [22]. A 350 °C heat treatment has been reported in other studies as a means of transforming the amorphous oxide to a crystalline Ti oxide [23, 24].

High-resolution XPS analyses indicated a 5.8 eV peak separation between the Ti $2p_{1/2}$ and Ti $2p_{3/2}$ peaks for the Ti samples prior to immersion and the TiO_2 single crystal standard. The peak separation for Ti surfaces after immersion was also in close agreement with the TiO_2 single crystal standard. In concurrence with other investigators, this peak separation and peak position indicated the presence of TiO_2, with an oxidation state of 4 + [25, 26]. However, differences in the FWHM value of Ti $2p_{3/2}$ peak for the Ti sample and TiO_2 single crystal were observed. The Ti samples exhibited a broader Ti $2p_{3/2}$ peak (FWHM = 1.3) than the TiO_2 single crystal (FWHM = 1.1), suggesting an amorphous oxide layer. This has been confirmed by other investigators who have shown FWHM values of 1.3 for Ti $2p_{3/2}$ for TiO_2 films produced by reactive ion plating [25].

From the O 1s high-resolution spectra prior to immersion in solution, component A is attributed to

bulk TiO_2. However, controversies arise in assigning the two higher binding energy O 1s components. The two carbon components (286.1 eV and 288.1 eV) observed in the high-resolution C 1s spectra were suggested to correspond to C–O and C=O species, respectively, and thus contributed to the two oxygen components at higher binding energies [26, 28–30]. Other investigators have reported that these two higher energy oxygen components are contributions from hydroxyl groups and chemisorbed water [31].

After immersion in α-MEM, relative concentrations of components A and B of the O 1s spectrum were observed to change with time, an indication of a dynamic surface. It was not surprising to observe a decrease in the concentration of component A, since this component was attributed to the bulk TiO_2. This decrease in the concentration of component A was the result of the increasing Ca–P deposition, and thus the coverage of the TiO_2 layer. The increase in the relative concentration of component B indicated contributions from the solution, thereby causing a change in the surface composition. The presence of another species such as PO_4 in addition to the initial small amount of C–O species was suggested. Comparing the O 1s spectra for the brushite and hydroxyapatite standards confirmed that component B was primarily due to PO_4 species. The relative concentration of component C was not statistically changed during immersion, suggesting that the deposition of inorganic constituents did not contribute to this component. Thus, component C was primarily due to either C=O and/or possibly hydroxyl species.

After immersion in the α-MEM solution, Ca and P were observed on the Ti surface. With an increase in immersion time, the concentration of Ca and P increased. In concurrence with the O 1s spectrum, the P 2p spectrum also indicated a dynamic surface during immersion. The high-resolution P 2p spectra was asymmetric after 6 days immersion and was resolved into two components. The peak positions of these two components were more similar to the peak positions of the brushite standard than the hydroxyapatite standard. This suggested that after 6 days immersion, the Ca–P compounds on the Ti surfaces exhibited a chemistry similar to brushite. The phosphorus deposited on the Ti surfaces at peak positions 133.1 eV and 134.3 eV corresponded to HPO_4^{2-} and $H_2PO_4^-$ species, respectively. Furthermore, the initially higher atomic concentration of phosphorus as compared to calcium ions has been similarly observed by other investigators [32]. It has been suggested that the passive dissolution of oxide in solution may possibly cause the reaction of phosphorus ions with the Ti surface, thereby resulting in the initially high phosphorus adsorption. This phosphorus adsorption has been similarly observed during the change in the kinetics of passive dissolution behaviour of titanium oxide [33].

As observed during FTIR analyses, a broad PO_4 absorbance band was exhibited in the range 900 cm^{-1} to 1200 cm^{-1}. In concurrence with the XPS analyses, this broad band indicated an amorphous fine crystalline Ca–P compound on the Ti surfaces [34, 35]. In agreement with other investigations, the formation of amorphous fine crystalline Ca–P compound is speculated to be dependent upon the crystallinity of the sample surface [35]. However, since XPS analyses have indicated an amorphous fine crystalline compound having chemistry similar to brushite, these compounds could be a precursor for the formation of brushite or a mixture of brushite and oxyhydroxyapatite [36]. This is in agreement with other studies in which a mixture of brushite and neutral Ca–P compounds are reported to be amorphous fine crystalline as determined by X-ray diffraction during initial precipitation [37]. The transformation of amorphous fine crystalline Ca–P to crystalline Ca–P phases such as brushite have also been reported to require factors such as the presence and concentrations of calcium, phosphorus and magnesium ions, pH and temperature [36].

5. Summary

The overall success of a Ti implant is dependent on the surface properties, which may include the composition and structure of ionic deposits on the implant surface. In this study, an amorphous TiO_2 layer was observed on the Ti surface. XPS analyses revealed that the oxide surface is not purely TiO_2, but also contains contamination such as hydrocarbons, C–O, C=O and hydroxyl species. In the presence of α-MEM, dynamic change in the surface chemistry were observed. Ions such as phosphorus were initially deposited in greater concentration than Ca ions, and with time, these ions were increasingly deposited as amorphous fine crystalline Ca–P compounds, with Ca/P ratio of 1.2 after 12 days immersion. Comparing the P 2p peak positions to known standards, these amorphous fine crystalline Ca–P deposits after 6 days immersion were similar to brushite in chemistry. A greater understanding is required of the nature and transformation of amorphous Ca–P compounds, and their influence on tissue response *in vivo*.

Acknowledgement

This study is supported by the National Science Foundation.

References

1. T. ALBREKTSSON and M. JACOBSSON, *J. Prosth. Dent.* **57** (1987) 597.
2. L. SENNERBY, P. THOMSEN and L. E. ERICSON, in Transactions of the Society for Biomaterials, Orlando, FL, May 1990 (Society for Biomaterials, Birmingham, Alabama, 1990) p. 82.
3. D. F. WILLIAMS and G. MEACHIM, *J. Biomed. Mater. Res. Symp.* **5** (1974) 1.
4. G. D. WINTER, *ibid.* **5** (1974) 11.
5. S. B. GOODMAN, P. ASPENBERG, Y. SONG, A. DOSHI, D. REGULA and L. LIDGREN, in Transactions of the Society for Biomaterials, Birmingham, AL, April 1993 (Society for Biomaterials, Minneapolis, MN, 1993) p. 240.
6. B. KASEMO and J. LAUSMAA, *CRC Crit. Rev. Biocomp.* **2** (1986) 335.
7. J. D. ANDRADE, in "Surface and interfacial aspects of biomedical polymers", Vol. 2, edited by J. D. Andrade (Plenum Press, New York, 1985) p. 1.

8. T. A. HORBETT and J. L. BRASH, in "Proteins at interface", edited by J. L. Brash and T. A. Horbett (ACS, Washington, 1987) p. 1.
9. J. KELLER, WM. J. DOUGHERTY, G. R. GROTENDORST and J. P. WIGHTMAN, *J. Adhesion* **28** (1989) 115.
10. J.-E. SUNDGREN, P. BODO and I. LUNDSTROM, *J. Colloid Interface Sci.* **110** (1986) 9.
11. D. McQUEEN, J.-E. SUNDGREN, B. IVARSSON, I. LUNDSTROM, B. AFEKENSTAM, A. SVENSSON, P.-I. BRANEMARK and T. ALBREKTSSON, in "Clinical applications of biomaterials", edited by A. J. C. Lee, T. Albrektsson and P.-I. Branemark (Wiley, New York, 1982) p. 179.
12. A. L. BOSKEY and A. S. POSNER, *Mater. Res. Bull.* **9** (1974) 907.
13. E. D. EANES, J. D. TERMINE and M. U. NYLEN, *Calcif. Tissue Res.* **12** (1973) 143.
14. J. C. HEUGHEBAERT and G. MONTEL, *Calcif. Tissue Int.* **34** (1984) 103.
15. J. C. KELLER, R. A. DRAUGHN, J. P. WIGHTMAN, W. J. DOUGHERTY and S. D. MELETIOU, *Int. J. Oral Maxillofacial Imp.* **5** (1990) 360.
16. C. KLAUBER, L. J. LENZ and P. J. HENRY, *ibid.* **5** (1990) 264.
17. J. LAUSMAA, B. KASEMO and S. HANSSON, *Biomaterials* **6** (1985) 23.
18. K. E. HEALY and P. DUCHEYNE, *J. Biomed. Mater. Res.* **26** (1992) 319.
19. J. L. ONG, L. C. LUCAS, G. N. RAIKAR and J. C. GREGORY, *Appl. Surf. Sci.* **72** (1993) 7.
20. C. M. MICHAELS, J. C. KELLER and C. M. STANFORD, *J. Oral Implant.* **17** (1991) 132.
21. T. ALBREKTSSON and H.-A. HANSSON, *Biomaterials* **7** (1986) 201.
22. P. TENGVALL and I. LUNDSTROM, *Clin. Mater.* **9** (1992) 115.
23. L. S. HSN, R. RUJKORAKARN, J. R. SITES and C. Y. SKE, *J. Appl. Phys.* **59** (1986) 3475.
24. M. LOTTIANX, C. BOULESTEIX, G. NIHOUL, F. VARNIER, F. FLORY, R. GALINDO and E. PELLETIER, *Thin Solid Films* **170** (1989) 107.
25. K. BANGE, C. R. OTTERMANN, O. ANDERSON, U. JESCHKOWSKI, M. LAUBE and R. FEILE, *ibid.* **197** (1991) 279.
26. J. LAUSMAA, B. KASEMO and H. MATTSSON, *Appl. Surf. Sci.* **44** (1990) 133.
27. C. D. WAGNER, W. M. RIGGS, L. E. DAVIS and J. F. MOULDER, in "Handbook" of X-ray photoelectron spectroscopy", edited by G. E. Muilenberg (Perkin-Elmer Corporation, MN, 1979).
28. W. F. STICKLE and J. F. MOULDER, *J. Vac. Sci. Technol.* **A9** (1991) 1441.
29. Perkin-Elmer Physical Electronics, in "Introduction to polymer studies with ESCA", Applications Note No. 7905, Aug 30, 1979.
30. T. J. LENK, B. D. RATNER, R. M. GENDREAU and K. K. CHITTUR, *J. Biomed. Mater. Res.* **23** (1989) 549.
31. N. S. McINTYRE and T. C. CHEN, in "Practical surface analysis", 2nd Edn, Vol. 1, edited by D. Briggs and M. P. Seah (Wiley, New York, 1990) p. 501.
32. T. HANAWA and M. OTA, *Biomaterials* **12** (1991) 767.
33. P. DUCHEYNE and K. HEALY, in "The bone-biomaterial interface", edited by J. E. Davis (University of Toronto Press, Toronto, 1991) p. 62.
34. J. L. ONG and L. C. LUCAS, *Biomaterials* (in press).
35. N. PLESHKO, A. BOSKEY and R. MENDELSOHN, *Biophys. J.* **60** (1991) 786.
36. R. Z. LeGEROS, in "Calcium phosphates in oral biology and medicine" (Karger, New York, 1991) p. 46.
37. E. D. EANES, P. H. GILLESEN and A. S. POSNER, *Nature* **208** (1965) 365.

Received 11 October 1993
and accepted 31 March 1994